

An improved demodulation method for image sensor based visible light communication using sparse estimation technique

1st Yuki OHIRA
Sumitomo Heavy Industries, Ltd.
Yokosuka, Japan
yuki.ohira@shi-g.com

2nd Tomohiro YENDO
Nagaoka University of Technology
Nagaoka, Japan
yendo@vos.nagaokaut.ac.jp

Abstract—Visible Light Communication (VLC) is a promising research field due to the versatility and ubiquity of Light Emitting Diodes (LEDs). In this study, we focus on VLC systems with image-sensor as a receiver for intelligent transport systems (ITS). The design of efficient demodulation methods for these systems remains a significant challenge, especially given the demand for a balance between computational complexity and demodulation performance. This paper introduces a demodulation method for the VLC systems that takes advantage of sparse estimation techniques. The proposed approach uses Orthogonal Matching Pursuit (OMP) coupled with Maximum-Likelihood Detection (MLD) to improve upon the performance of linear detectors such as Zero-Forcing and Minimum-Mean-Square-Error. Using a sparse characteristics, the OMP/MLD technique provides a refined estimation of transmitted signals. This method is showcased through numerical simulations and lab-based experiments, demonstrating improved performance compared to traditional techniques. This research contributes to the ongoing efforts in optimizing VLC systems and offers an enhancement in the demodulation process of Image-Sensor Communication systems.

Index Terms—VLC, OWC, ITS, ISC, MIMO

I. INTRODUCTION

Visible Light Communication (VLC) represents a rapidly evolving field in optical wireless communication, leveraging the blinking lights within the visible spectrum to transmit information [1]. The growing interest in VLC can largely be attributed to the increasing availability of Light-Emitting Diodes (LEDs), which has significant implications for the communication sector [2].

LEDs possess distinctive attributes in various aspects, such as energy efficiency, ecological impact, low-voltage operation, and high visibility. In addition, the semiconductor structure of LEDs allows for easy brightness control, which significantly improves their suitability for communication devices. Due to these diverse advantages, LEDs have captured the attention of researchers in the communications field, leading to a growing body of work focused on the development of LED-based VLC systems for signal transmission. This study continues in this direction, aiming to develop novel methods of signal demodulation that will enhance the performance and reliability of VLC systems [3].

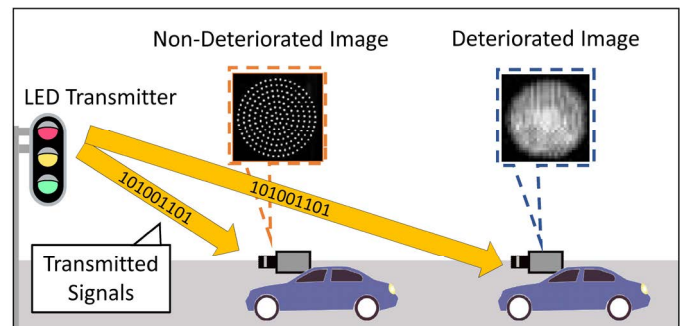


Fig. 1. ISC for infrastructure-to-vehicle communication. The quality of an image captured at a long distance will be deteriorated.

The choice of the receiver in VLC systems is crucial, typically offering options such as photo-diode arrays or image sensors. A photo-diode array transforms the received light into an electrical current, achieving light detection at rate on the order of tens of MHz. Alternatively, an image sensor can also serve as a receiver for transmitted light signals, defining what is known as an Image-Sensor Communication (ISC) system.

While ISC systems often exhibit transmission speeds inferior to those equipped with photo-diode receivers, primarily due to the image sensor's limited frame rate, they provide unique advantages in scenarios involving multiple LED transmitters [4]. Specifically, if each LED is individually modulated, an image sensor can simultaneously capture signals from multiple LED transmitters. Subsequently, the pixel values corresponding to each transmitter can be distinguished in the captured image [5]. Moreover, an image sensor can discern between transmitted optical signals and ambient noise sources, such as sunlight, further enhancing the utility and robustness of ISC systems.

This paper explores the ISC system designed to support an Intelligent Transport System (ITS) [6]. The proposed system utilizes an LED traffic light as a transmitter and an image sensor, installed on vehicles, as the receiver [7]. In this context, the vehicle-mounted image sensor captures the signals emitted by patterns of LEDs embedded in traffic lights. Each LED

traffic light comprises approximately a hundred individual LEDs, with the intensity of each being modulated independently [8]. Pixel values corresponding to each individual LED are extracted from the captured images, from which the signals are subsequently demodulated. This arrangement facilitates parallel data transmission, achieved by emitting signals through multiple LEDs simultaneously. Parallel data transmission significantly enhances the transmission rate of ISC systems [9].

A commonly cited challenge associated with ISC systems is the dependence of image quality on communication distance (Fig. 1). In a scenario where an ISC system transmits data in parallel using multiple LEDs, it is crucial for the receiver to accurately identify the position and brightness of each LED in the captured image [10]. However, as the communication distance lengthens, the captured image tends to be deteriorated due to defocusing, each LED occupies fewer pixels in the image, and the light from each LED diffuses over extended distances, resulting in each LED's light signal influencing the neighboring pixels. This effect complicates the receiver's task of correctly identifying the LED positions and their corresponding brightness levels, posing a significant hurdle in the accurate demodulation of signals [12]. This paper proposes a solution to this challenge, aiming to optimize the demodulation process in ISC systems for improved performance and reliability.

In a system that uses parallel data transmission, data is allocated to each LED on the transmitter. Binary bits of "1" or "0" represented by the LED states of being either "ON" or "OFF", a process known as On-Off Keying (OOK) modulation. The data recovery process relies on the brightness of each pixel corresponding to the individual LEDs.

Figure 2 illustrates a system model of the ISC system. In this model, the transmitted signals captured by the image-sensor, and the pixel values corresponding to each LED in the captured image are expressed as the summation of diffused light from each transmitting LED.

In the quest to enhance the demodulation performance of ISC systems, several traditional demodulation techniques have been attempted. The Maximum-Likelihood Detector (MLD), for instance, carries out an exhaustive search within the entire solution space [11]. However, this approach is frequently deemed impractical due to its substantial computational complexity, which ordinarily escalates exponentially in relation to the number of LEDs involved in the system. On the other hand, linear detectors such as the Minimum-Mean-Square-Error (MMSE) and Zero-Forcing (ZF) detectors present a lower degree of complexity [12]. Despite this advantage, their performance is generally below the ideal benchmark. In light of these constraints, the development of new demodulation methods, capable of achieving an improved balance between performance and complexity, is of paramount importance for ISC systems. With this objective in mind, our study proposes a novel demodulation technique. It is specifically designed to enhance the performance of ISC systems without increasing computational complexity, thus addressing a key challenge in

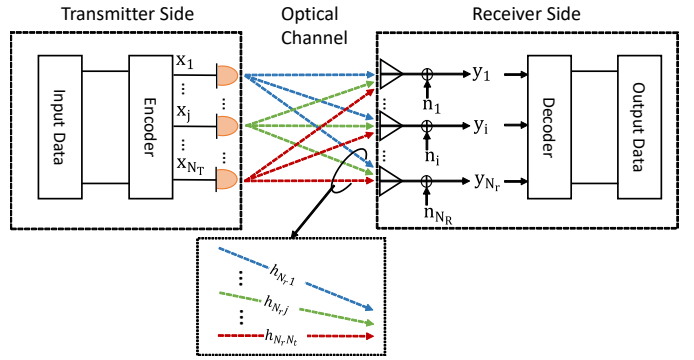


Fig. 2. System model of ISC.

this field.

Our approach introduces sparse error recovery techniques [13] [14] as a demodulation method for ISC systems. The detectors leverage the inherent sparsity of a residual vector to refine the results obtained by a low-complexity linear detector, such as ZF or MMSE. More specifically, given the known channel matrix $\mathbf{H} \in \mathbb{R}^{N_R \times N_T}$, where N_R is the number of pixels and N_T is the number of LEDs, the transmitted signal vector $\{\mathbf{x} = (x_1, x_2, \dots, x_{N_T})^T \in \mathbb{R}^{N_T} | x_i \in \{0, 1\}, i = 1, 2, \dots, N_T\}$ is first detected using either ZF or MMSE, along with a slicing function. By subtracting the product of the estimated transmitted signal vector $\hat{\mathbf{x}} \in \mathbb{R}^{N_T}$ and the channel matrix \mathbf{H} from the original received signal $\mathbf{y} (= \mathbf{H}\mathbf{x} + \mathbf{n}) \in \mathbb{R}^{N_R}$, we obtain a residual vector $\hat{\mathbf{y}} \in \mathbb{R}^{N_R}$.

$$\hat{\mathbf{y}} = \mathbf{y} - \mathbf{H}\hat{\mathbf{x}} = \mathbf{H}(\mathbf{x} - \hat{\mathbf{x}}) + \mathbf{n} = \mathbf{H}\mathbf{e} + \mathbf{n}. \quad (1)$$

where $\mathbf{e} (= \mathbf{x} - \hat{\mathbf{x}}) \in \mathbb{R}^{N_T}$ is a sparse error vector and $\mathbf{n} \in \mathbb{R}^{N_R}$ is the additive white Gaussian noise (AWGN) vector. This operation results in a sparse ISC system due to the generally small Bit Error Rates (BERs) achieved by the underlying linear detector in practical Signal-to-Noise Ratio (SNR) regimes. Afterwards, a sparse error detector is employed to acquire a sparse error vector \mathbf{e} , which is then used to refine $\hat{\mathbf{x}}$. This approach capitalizes on the power of sparse estimation techniques to recover errors in the initial estimation and enhance the performance and accuracy of the demodulation process while maintaining a manageable computational complexity.

II. DEMODULATION METHOD BASED ON SPARSE ERROR RECOVERY

With the conventional ZF/MMSE method, the received signals are subjected to filtering via a matrix \mathbf{W} , which according to the ZF and MMSE criteria, is respectively given by

$$\mathbf{W}_{ZF} = (\mathbf{H}^T \mathbf{H})^{-1} \mathbf{H}. \quad (2)$$

$$\mathbf{W}_{MMSE} = (\mathbf{H}^T \mathbf{H} + \frac{1}{\sigma^2} \mathbf{I})^{-1} \mathbf{H}. \quad (3)$$

where σ^2 denotes an input signal-to-noise ratio, and \mathbf{I} is an $N_R \times N_T$ identity matrix.

Subsequently, the estimated signal vector $\hat{\mathbf{x}}$ is derived via a hard decision of $\mathbf{W}\mathbf{y}$. This can be expressed as $\hat{\mathbf{x}} = Q(\mathbf{W}\mathbf{y})$ for both ZF and MMSE, where $Q(\cdot)$ is a slicing function mapping each element to either “0” or “1”, given the OOK modulation in use. Through this process, our method utilizes the ZF and MMSE criteria to effectively demodulate the transmitted signals.

When conventional ZF or MMSE method are applied to the system for signal demodulation, it becomes evident that their outputs closely resemble the original transmitted vector \mathbf{x} in practical SNRs. However, they do not always produce an exact match. This discrepancy can potentially introduce errors into the system. To apply the sparse error recovery technique, we convert the non-sparse system into sparse one. Conventional detection together with the symbol slicing serves our purpose since the estimated signal vector is roughly accurate, and hence, the resulting error vector can be modeled as sparse signal.

The error vector \mathbf{e} is generally small, which lends itself to be modeled as a sparse vector. To illustrate, let’s consider a scenario where the dimension of the signal vector \mathbf{x} is 9. Suppose the transmitted signals \mathbf{x} are represented as $(0, 1, 1, 0, 0, 1, 1, 0, 1)$, and the estimated signals denoted by $\hat{\mathbf{x}}$ are $(0, 1, 1, 0, 1, 1, 1, 0, 0)$. In this case, the sparse error vector $\mathbf{e}(=\mathbf{x}-\hat{\mathbf{x}})$ becomes $(0, 0, 0, 0, -1, 0, 0, 0, 1)$. The elements of \mathbf{e} take values from a finite alphabet $\mathbb{A} = \{-1, 0, +1\}$. Here, a non-zero value “-1” or “+1” symbolizes a detection error. Indeed, since most elements of \mathbf{e} are expected to be “0”, we can consider \mathbf{e} as a sparse vector. The assumption of sparsity in this context is advantageous as it allows us to employ sparse estimation techniques. These techniques excel in identifying and extracting non-zero elements from a sparse vector, making them particularly suitable for estimating the error vector \mathbf{e} . The sparse estimation problem is written as below.

$$\begin{aligned} \hat{\mathbf{e}} &= \underset{\mathbf{e} \in \mathbb{A}}{\operatorname{argmin}} \|\hat{\mathbf{y}} - \mathbf{H}\mathbf{e}\|_2^2 \\ &\text{subject to } \|\mathbf{e}\|_0 \leq K. \end{aligned} \quad (4)$$

where $K (\ll N_T)$ denotes a predefined number of non-zero elements. Several algorithms exist that can solve this equation. However, in this paper, we specifically introduce a sparse estimation method that integrates the Orthogonal Matching Pursuit (OMP) [15] and the MLD method to optimize the estimated error vector $\hat{\mathbf{e}}$ [16].

OMP is a widely adopted sparse estimation technique that is particularly well-suited for the task of sparse error vector estimation. OMP is an iterative greedy algorithm, which means it makes the locally optimal choice at each stage with the hope that these local choices will lead to a global optimum. In each iteration of OMP, the algorithm selects the atom from the channel matrix most correlated with the current residual. This selected atom is then included in the active set, and the signal estimated is updated by projecting the residual signal onto the subspace spanned by the active set. The residual is then updated by removing the component of the residual signal that

lies in the direction of the selected atom. This process repeats iteratively until a stopping criterion is met, which could be a predetermined sparsity level or a threshold for the residual’s norm.

The MLD method effectively converts the estimated error vector into quantized symbols, facilitating a more reliable signal demodulation. In this context, the complexity of the MLD is restricted to $\mathcal{O}(3^K)$ which is generally smaller compared to the original MLD method ($\mathcal{O}(2^{N_T})$). The MLD convert these non-zero elements into one of \mathbb{A} . This integrated OMP/MLD approach offers an effective and efficient solution for demodulating signals in ISC systems, offering a promising balance between performance and computational complexity. The pseudo-code for the algorithm is given in Algorithm 1.

Algorithm 1 OMP/MLD Method for Sparse Error Vector Estimation

Require: Channel matrix \mathbf{H} , residual signal $\hat{\mathbf{y}}$, number of non-zero elements K
Ensure: Estimated error vector $\hat{\mathbf{e}}$

- 1: $\hat{\mathbf{e}} \leftarrow \mathbf{0}, \mathbf{r} \leftarrow \hat{\mathbf{y}}$ ▷ Initialization
- 2: $S \leftarrow \{\}$ ▷ Index set for selected atoms
- 3: **for** $k = 1$ to K **do** ▷ Main loop
- 4: $i \leftarrow \underset{i \notin S}{\operatorname{argmax}} |\mathbf{H}_i^T \mathbf{r}|$ ▷ Find the atom most correlated with the residual
- 5: $S \leftarrow S \cup \{i\}$ ▷ Update the index set
- 6: $\hat{\mathbf{e}} \leftarrow \underset{\hat{\mathbf{e}} \in \mathbb{A} = \{0, \pm 1\}}{\operatorname{argmin}} \|\hat{\mathbf{y}} - \mathbf{H}_S \hat{\mathbf{e}}\|_2^2$ ▷ Apply MLD to estimate the discrete signal over the selected atoms
- 7: $\mathbf{r} \leftarrow \hat{\mathbf{y}} - \mathbf{H}\hat{\mathbf{e}}$ ▷ Update the residual
- 8: **end for**

return $\hat{\mathbf{e}}$

From the estimated error signals $\hat{\mathbf{e}}$, we can enhance the initially estimated signal $\hat{\mathbf{x}}$ using the following equation.

$$\hat{\hat{\mathbf{x}}} = \hat{\mathbf{x}} + \hat{\mathbf{e}}. \quad (5)$$

This equation shows how our method refines the initial signal estimate by adding the estimated error vector. The revised signal $\hat{\hat{\mathbf{x}}}$, thus captures a more accurate depiction of the transmitted data, thereby improving the demodulation performance of the ISC system.

III. SIMULATION RESULT

The results of the simulation have been presented in this section, conducted to validate the demodulation performance of the proposed method. The conditions for the simulation are outlined in Table I. The LED array for the transmitter is arranged as an 8×8 matrix, and the modulation scheme used is OOK. Consequently, the transmitter is able to simultaneously send 64 bits of data. The simulation presupposes a uniform luminance value for all the LEDs. A Gaussian filter is utilized to blur the images, which is formulated on the basis of the 2D Gaussian function described by (6).

TABLE I
SIMULATION CONDITIONS.

Modulation method	On-Off-Keying (OOK)
Number of LEDs	64 (8×8 matrix)
Filtering	Gaussian filter
SNR	10–25 in dB
Simulation iterations	10,000 for each SNR

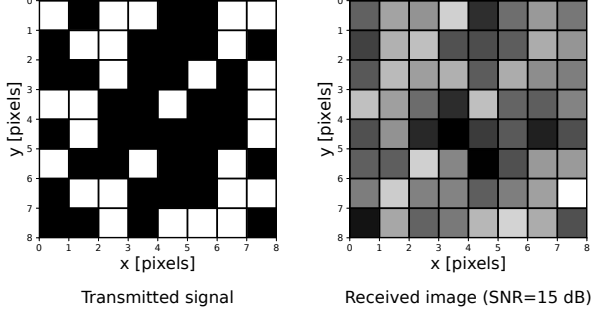


Fig. 3. A sample of a transmitted signal (left) and the corresponding received image (right) generated under the described simulation condition.

$$h_g(p, q) = \frac{1}{2\pi\sigma_g^2} \exp\left(-\frac{p^2 + q^2}{2\sigma_g^2}\right). \quad (6)$$

where σ_g^2 (> 0) is the variance of the Gaussian function, and p and q are the vertical and horizontal coordinates, of a pixel's distance from the origin. The optical channel matrix in the simulations is calculated using (6). The image is assumed to be affected by AWGN, which is added to each pixel of the image. The SNR ranges from 10 dB to 25 dB. Figure 3 shows a sample case of transmitted signal and its corresponding received image at 15 dB. To examine the effectiveness of sparseness, the number of sparse elements K in the error vector was varied between 3 to 5. The simulation was repeated 10,000 times and the BER was noted down for various SNR values. This simulation process helps to confirm the practical effectiveness and performance of the OMP/MLD demodulation method.

Equation (7) shows a slicing function for the OMP. This slicing function is an integral part of the OMP, used to convert continuous-valued estimates to discrete-valued symbols.

$$Q(x) = \begin{cases} 1, & \text{if } 0.5 \leq x \\ -1, & \text{if } x \leq -0.5 \\ 0, & \text{otherwise} \end{cases} \quad (7)$$

Figure 4 visualizes the BERs of the MMSE method, the OMP and the OMP/MLD method for $K=3$ and 5. The OMP/MLD method consistently delivers superior BER performance compared to the other methods at any given SNR. More specifically, at SNR of 25 dB, errors are observed in the MMSE method. The OMP method with $K=3$ and 5 begins to show errors at SNR of 22 dB and 23 dB. For the OMP/MLD method with $K=3$ and 5, errors start at SNR of 22 dB. The BER performance of the OMP/MLD method enhances

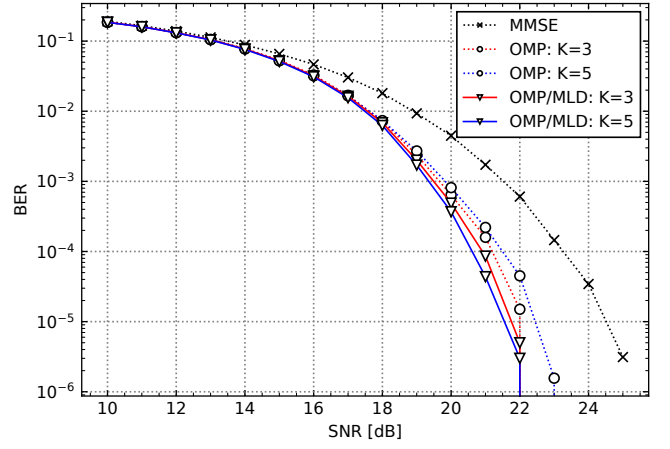


Fig. 4. Simulation Results: BER performance of the proposed OMP/MLD, OMP and MMSE method plotted against SNR.

as the number of sparse elements, K , increases from 3 to 5. Conversely, the BER performance of the OMP method is improved as K is decreased from 5 to 3. This discrepancy in performance can be attributed to the quantization methods employed by each approach. The OMP method leverages hard thresholding (7) for quantization, which may result in a misinterpretation of certain elements in the error vector, particularly when the sparsity level is lower. This misinterpretation could lead to a decline in the BER performance. On the other hand, the OMP/MLD method implements the MLD technique for quantization, which optimizes the accuracy of the error vector interpretation.

The simulation result demonstrates that the utilization of MLD for signal detection outperforms the standalone OMP method, with a marginal increase in computational complexity. These findings verify the applicability of the error refinement technique for demodulation in ISC.

IV. EXPERIMENTAL RESULT

In order to further confirm the effectiveness of the proposed demodulation method, we conducted lab-based experiment to evaluate BER performance.

Table II lists the specifications of the transmitter and the receiver. The transmitter and the receiver were held still and arranged face-to-face in a straight line. The experiment was conducted in a darkroom, so that neither device was affected by noise from ambient light such as the sun. But both devices were still affected by electronics shot noise.

The LED transmitter consists of 16 LEDs arranged in a 4×4 square matrix and an encoder using FTDI MorphIC-II board. The LEDs are spaced at 20 mm intervals. The transmitted data is segmented into packets, each containing header and data components. For the header, the transmitter sequentially illuminates the 16 LEDs to establish the correct position of each LED in the images recorded at the receiver, also transmitting known signals for the estimation of optical

TABLE II
EQUIPMENT SPECIFICATIONS

Transmitter	
LED	Cree CLP6C-FKB-CK1P1G1BB7R3R3
LED driver	Texas Instruments TLC5922
Control board	FTDI Morph-IC-II (Altera FPGA)
Receiver	
Camera	IDS UI-3250ML-M-GL
Camera lens	SPACECOM JHF8M-MP

TABLE III
EXPERIMENTAL PARAMETERS

Modulation method	On-Off-Keying (OOK)
LED frequency	150 Hz
Frame rate	150 fps
Number of LEDs	16
Number of images	10,000 for each SNR
Transmission data	Random bits (0 or 1)
Distance	5.3 m
Location	Darkroom (static condition)
Image size	42×36 pixels
Image color	Grayscale

channel parameters. For data transmission, pseudo-random data modulated by OOK is utilized.

Table III outlines the experimental parameters. The receiver first records images of the transmitted LED light, locating the beginning of the header part to determine the position of each LED in the image. The transmitter then sends data in 10,000 LED patterns, totalling 160,000 transmitted bits. Subsequently, the channel parameters are calculated to reconstruct the channel matrix based on the captured images. Finally, the receiver applies the proposed demodulation method using the estimated channel matrix to recover the data. Figure 5 provides an example of actual images captured from 4 × 4 LED array.

In our experimental setup, we further incorporate the BER performance of the original MLD method into our comparative analysis. This allows us to not only measure the effectiveness of our proposed OMP/MLD approach but also observe its performance relative to the MLD method, which is well-regarded for its optimal performance despite its high computational demand.

Figure 6 presents the experimental BER performance with the same demodulation methods as those used in the simulation. In the real-world setting, at SNR of 17.5 dB, errors are observed across all methods except for the MLD method. The OMP/MLD method with $K=3$ and 5 exhibits superior BER performance compared to the OMP and MMSE methods at any SNR level. This suggests that our proposed approach not only works well under controlled simulation conditions but also demonstrates strong performance in more complex, real-world environments. The MLD method showcases superior BER performance as compared to the proposed method. This can be explained by understanding that the MLD method employs exhaustive searching over the entire signal space to find the optimal solution. This approach, while computationally expensive, ensures that the solution obtained is likely the

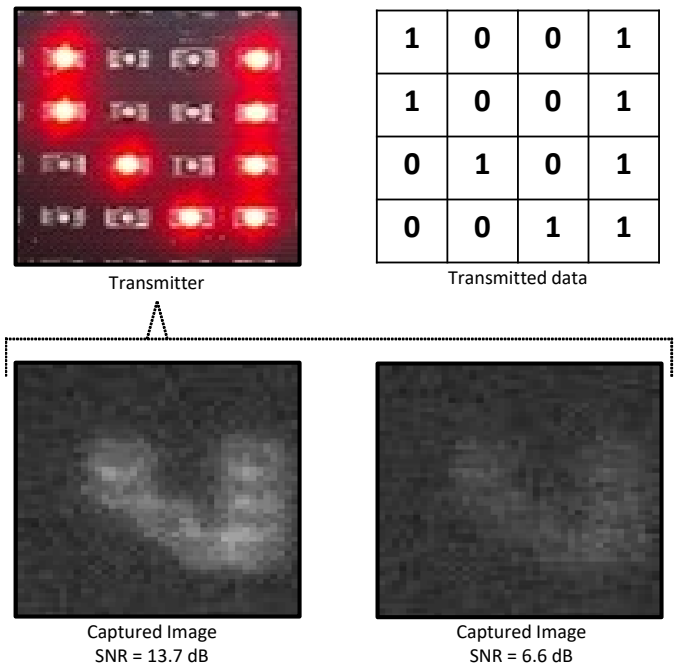


Fig. 5. LED transmitter, corresponding signal pattern, and actual captured images at two different SNRs [dB].

global optimum, hence the superior BER performance. In contrast, the OMP/MLD method is a hybrid approach that combines the greedy selection of OMP with the optimized search of MLD, but only within a limited subspace defined by the sparsity level. Therefore, while the OMP/MLD method achieves improved BER performance compared to the standalone OMP approach, it may not outperform the original exhaustive MLD method in terms of BER. Nevertheless, it is crucial to acknowledge that the computational complexity of the MLD method is significantly higher, making it less practical for real-time applications or systems with resource constraints. Hence, the proposed OMP/MLD method offers a balanced trade-off between performance and complexity, providing a promising solution for efficient signal demodulation in ISC systems.

In conclusion of the experiment, allowing the OMP to conduct additional iterations and integrating it with MLD emerges as a powerful and efficient approach. This strategy enhances the performance of ISC systems without an excessive increase in computational complexity, making it a promising solution for practical applications.

V. CONCLUSION

This paper has presented a demodulation method for ISC systems using a sparse error recovery technique. This method leverages the strengths of both the OMP and the MLD techniques to enhance signal demodulation performance in ISC systems. The proposed OMP/MLD approach proves effective in mitigating the inherent challenges of traditional methods such as high computational complexity (MLD) and limited

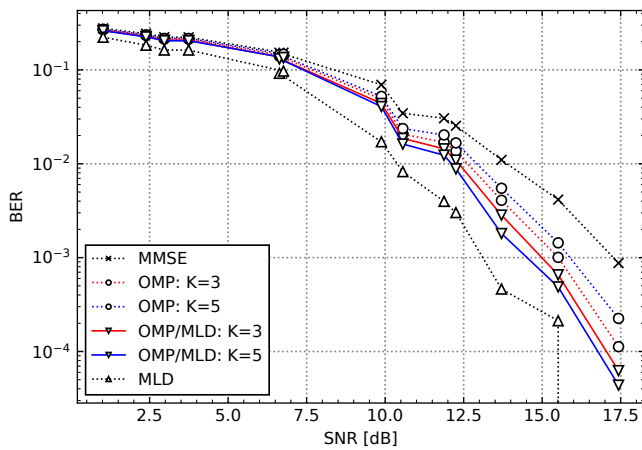


Fig. 6. Experimental Result: BER performance of the proposed OMP/MLD, OMP, MMSE and MLD method plotted against SNR.

performance (ZF and MMSE). The proposed method adapts well to the sparse nature of the error vector in an ISC system, thereby achieving superior performance. Our simulation and experimental results validate the effectiveness of the proposed approach. It consistently outperforms traditional methods across a range of SNR conditions, demonstrating its practical applicability. This study thus provides a promising solution to the challenge of balancing performance and computational complexity in ISC systems. Nevertheless, as the field of ISC continues to evolve rapidly, future research should continue to explore and refine this method, examine its performance under various real-world conditions, and integrate it with other emerging techniques to fully harness the potential of ISC systems.

REFERENCES

- [1] G. Pang, T. Kwan, H. Liu, and C.H. Chan, "LED wireless," *IEEE Industry Applications Magazine*, 8(1), 21–28, 2002.
- [2] P. Daukantas, "Optical wireless communications: the new "Hot spot"?", *Optics and Photonics News*, 25(3), 34–41, 2014.
- [3] L.U. Khan, "Visible light communication: applications, architecture, standardization and research challenges," *Digital Communications and Networks*, 3(2), 78–88, 2017.
- [4] T. Komine and M. Nakagawa, "Fundamental analysis for visible-light communication system using LED lights," *IEEE Transactions on Consumer Electronics*, 50(1), 100–107, 2004.
- [5] S. Arai, Y. Shiraki, T. Yamazato, H. Okada, T. Fujii, and T. Yendo, "Multiple LED arrays acquisition for image-sensor-based I2V-VLC using block matching," in *Proceedings of IEEE 11th Consumer Communications and Networking Conference*, 605–610, 2014.
- [6] T. Yamazato, I. Takai, H. Okada, T. Fujii, T. Yendo, S. Arai, M. Andoh, T. Harada, K. Yasutomi, K. Kagawa, and S. Kawahito, "Image-sensor-based visible light communication for automotive applications," *IEEE Communications Magazine*, 52(7), 88–97, 2014.
- [7] I. Takai, T. Harada, M. Andoh, K. Yasutomi, K. Kagawa, and S. Kawahito, "Optical vehicle-to-vehicle communication system using LED transmitter and camera receiver," *IEEE Photonics Journal*, 6(5), 1–14, 2014.
- [8] L. Zeng, D.C. O'Brien, H.L. Minh, G.E. Faulkner, K. Lee, D. Jung, Y. Oh, and E.T. Won, "High data rate multiple input multiple output (MIMO) optical wireless communications using white LED lighting," *IEEE Journal on Selected Areas in Communications*, 27(9), 1654–1662, 2009.

- [9] S. Arai, S. Mase, T. Yamazato, T. Endo, T. Fujii, M. Tanimoto, K. Kidono, Y. Kimura, and Y. Ninomiya, "Experimental on hierarchical transmission scheme for visible light communication using LED traffic light and high-speed camera," in *Proceedings of IEEE 66th Vehicular Technology Conference*, 2174–2178, 2007.
- [10] S. Nishimoto, T. Yamazato, H. Okada, T. Fujii, T. Yendo, and S. Arai, "High-speed transmission of overlay coding for road-to-vehicle visible light communication using LED array and high-speed camera," in *Proceedings of 3rd IEEE GLOBECOM Workshop on Optical Wireless Communications*, 1234–1238, 2012.
- [11] S. Arai, H. Matushita, Y. Ohira, T. Yendo, D. He, and T. Yamazato, "Maximum likelihood decoding based on pseudo-captured image templates for image sensor communication," *Nonlinear Theory and Its Applications*, IEICE, 10(2), 173–189, 2019.
- [12] Y. Ohira, S. Arai, T. Yendo, T. Yamazato, H. Okada, T. Fujii, K. Kamakura, "Novel Demodulation Scheme Based on Blurred Images for Image-Sensor Visible Light Communication," in *Proceedings of 6th IEEE Globecom Workshop on Optical Wireless Communications (OWC)*, 1–6, 2015.
- [13] J. W. Choi and B. Shim, "New Approach for Massive MIMO Detection Using Sparse Error Recovery," in *Proceedings of IEEE Global Communications Conference*, 3754–3759, 2014.
- [14] Y. Meslem, A. Aissa El Bey, M. Djeddou, "Improved sparse error recovery approach for detecting QAM signals in overloaded massive MIMO systems," in *Proceedings of IEEE Sensor Array and Multichannel Signal Processing Workshop*, 2020.
- [15] Y.C. Pati, R. Rezaifar, P.S. Krishnaprasad, "Orthogonal Matching Pursuit: Recursive Function Approximation with Applications to Wavelet Decomposition," in *Proceedings of Asilomar Conference*, 40–44, 1993.
- [16] S. Sparrer and R.F.H. Fischer, "Discrete Sparse Signals: Compressed Sensing by Combining OMP and the Sphere Decoder," *ArXiv*, abs/1310.2456, 2013.